Serotonergic Modulation of the Excitation-Inhibition Balance in the Visual Cortex

Estevão Carlos-Lima , Guilherme Shigueto Vilar Higa , Felipe José Costa Viana , Alicia Moraes Tamais , Fernando da Silva Borges , José Francis-Oliveira , Roberto De Pasquale *

Posted Date: 18 September 2023

doi: 10.20944/preprints202309.1107.v1

Keywords: 5-HT; visual cortex; E/I balance

Article

Serotonergic Modulation of the Excitation-Inhibition Balance in the Visual Cortex

Estevão Carlos-Lima [1], Guilherme Shigueto Vilar Higa [1,2,3], Felipe José Costa Viana [1], Alicia Moraes Tamais [1], Fernando da Silva Borges [4], José Francis-Oliveira [1] and Roberto De Pasquale [1,*]

[1] Laboratório de Neurofisiologia, Departamento de Fisiologia e Biofísica, Universidade de São Paulo, Butantã, São Paulo, SP 05508-000, Brasil
[2] Departamento de Bioquímica, Instituto de Química (USP), Butantã, São Paulo, SP 05508-900, Brasil
[3] Laboratório de Neurogenética, Universidade Federal do ABC, São Bernardo do Campo, SP 09210-580, Brasil
[4] Department of Physiology & Pharmacology, SUNY Downstate Health Sciences University, Brooklyn, NY 11203, US
* Correspondence: robertode@usp.br

Abstract: Serotonergic neurons constitute one of the main systems of neuromodulators, whose diffuse projections regulate the functions of the cerebral cortex. Serotonin (5-HT) is known to play a crucial role in the differential modulation of cortical activity related to behavioral contexts. Certain aspects of the 5-HT signaling framework hint at its potential role as a modulator of activity-dependent synaptic changes within the critical period of the primary visual cortex (V1). Cells of the serotonergic system are among the first neurons to differentiate and operate. During postnatal development, ramifications from raphe nuclei become massively distributed in the visual cortical area, remarkably increasing the availability of 5-HT for the regulation of excitatory and inhibitory synaptic activity. A substantial amount of evidence has demonstrated that synaptic plasticity at pyramidal neurons of the superficial layers of V1 critically depends on a fine regulation of the balance between excitation and inhibition (E/I). Therefore, 5-HT could play an important role in controlling this balance, providing the appropriate excitability conditions that favor synaptic modifications. In order to explore this possibility, the present work used in vitro intracellular electrophysiological recording techniques to study the effects of 5-HT on the E/I balance of V1 layer 2/3 neurons, during the critical period. Serotonergic modulation of the E/I balance has been analyzed on spontaneous activity, evoked synaptic responses, and long-term depression (LTD). Our results pointed out that the predominant action of 5-HT implies a reduction of the E/I balance. 5-HT promoted LTD at excitatory synapses while blocking LTD at inhibitory synaptic sites, thus shifting the Hebbian alterations of synaptic strength towards lower levels of E/I balance.

Keywords: 5-HT; Visual cortex; E/I balance

1. Introduction

Serotonin (5-HT) is among the most important endogenous neuromodulators in the central nervous system and the cerebral cortex receives extensive serotonergic projections originating from the raphe nuclei [1, 2]. 5-HT is widely diffusely from axonal varicosities, exerting its influence at a distance from its release sites by interacting with multiple receptors, primarily located on pyramidal neurons and interneurons[3, 4]. Within cortical regions, the predominant 5-HT receptors belong to the G-protein coupled receptor family, notably the 5-HT$_{1A}$, 5-HT$_{2A}$, and 5-HT$_{2C}$ subtypes[5-7]. The activation of these receptors leads to modulatory effects, with their specific roles varying based on distinct behavioral contexts[8]. Specifically, 5-HT is thought to establish functional connections between patterns of cortical activity and behaviorally relevant signals, facilitating selective alterations in cortical circuitry that are relevant for biological values[9, 10].

In the mammalian brain, serotonergic neurons are among the first cells to differentiate, leading to 5-HT availability to critically increase by the first three weeks of postnatal life [11-13]. 5-HT effects on

brain functions are thus remarkable during postnatal development when serotonergic modulation promotes activity-dependent long-lasting refinement of immature synaptic connections[11, 13-17]. In early life, the primary visual cortex (V1) receives a massive input of extensively ramified serotonergic projections reaching all cortical layers[18, 19]. In the V1 of kittens, 5-HT has been found to promote synaptic changes during the critical period of ocular dominance plasticity through activation of 5-HT_{2C} receptors [4, 20].

One of the key processes by which 5-HT may play its role in shaping V1 synaptic connectivity in early life involves the regulation of the excitation/inhibition balance (E/I) at superficial pyramidal neurons [21, 22]. Many evidences indicates pyramidal neurons indeed require tight modulation of the E/I balance for V1 to properly develop its physiological mature functions [23-26]. The outcome of the E/I balance fine regulation allows mature neurons to detect visual inputs, define the receptive field properties, and retransmit the appropriate information to higher-order cortical areas [23-31]. Between the third and the fourth week of rodent postnatal development, layer 2/3 becomes the main neuronal population of V1 where regulation of the E/I balance takes place [31-34]. Within this critical period, local excitatory and inhibitory circuits are thought to reach an optimal balance during which plasticity is facilitated and plays its role in shaping visual function [24-26]. However, the effects of 5-HT on the E/I balance of pyramidal neurons within this developmental context are still unclear.

The present study used in vitro intracellular recording techniques to investigate the effects of serotonergic modulation on E/I balance in three different contests: spontaneous synaptic activity, evoked synaptic transmission, and synaptic plasticity. Our results indicate that 5-HT reduces the E/I balance of spontaneous signals while maintaining this ratio constant in evoked responses. Furthermore, we show that 5-HT favors LTD in glutamatergic synapses while blocking LTD at GABAergic synapses, thereby promoting Hebbian plastic modifications at lower levels of the E/I balance.

2. Results

2.1. Serotonin decrease the E/I balance of spontaneous synaptic currents

As a first step of our work, we investigated the effects of 5-HT on glutamatergic activity of layer 2/3 neurons through the recording of spontaneous excitatory postsynaptic currents (sEPSCs). We first recorded the sEPSCs without 5-HT (control condition) and subsequently, 5-HT (50 μM) was applied in the bath for 10 minutes. Figure 1A shows two examples of recording traces with and without 5-HT. To evaluate the effects of 5-HT on excitatory synaptic activity, we analyzed the sEPSCs amplitude, frequency, and IEI (the time interval between a postsynaptic event and the previous one). We found that 5-HT reduced the mean amplitude of sEPSCs by approximately 10 pA and this difference was statistically significant (Figure 1B-C: 10 cells; Control, 29.58 ± 2.90 pA; 5-HT, 22.54 ± 0.72 pA; $p = 0.0432$, based on a paired t-test). However, when we compared the 5-HT and the control condition (without 5-HT), no significant differences were found related to the frequency (Figure 1D: 10 cells; Control, 1.56 ± 0.27 Hz; 5-HT, 2.36 ± 1.00 Hz; $p = 0.9219$, based on a Wilcoxon signed-rank test), nor any difference was observed when measuring the IEI values (Figure 1E: 10 cells; Control, 867.87 ± 194.78 ms; 5-HT, 980.07 ± 292.09 ms; $p = 0.5566$, based on a Wilcoxon signed-rank test).

In order to define a profile of 5-HT effects on the balance between excitation and inhibition (E/I ratio), we next investigated GABAergic activity by recording spontaneous postsynaptic inhibitory currents (sIPSCs). The sIPSCs were first recorded without 5-HT (control condition) and subsequently, 5-HT (50 μM) was applied in the recording chamber for 10 minutes. Figure 2A shows two example traces, one cell treated with 5-HT and another cell in the control condition. The effects of 5-HT on spontaneous GABAergic activity were analyzed by quantifying the amplitude, the mean frequency, and the IEI of sIPSCs. No significant differences were found for the amplitude (Figure 2B: 10 cells; Control, 41.70± 3.33pA; 5-HT, 45.77 ± 3.62 pA; $p = 0.3958$, based on a Wilcoxon signed-rank test). However, when we analyzed the frequency and the IEI, we observed significant differences. 5-HT increased the mean frequency of inhibitory synaptic events (Figure 2C: 10 cells; Control,

Preprints (www.preprints.org) | NOT PEER-REVIEWED | Posted: 18 September 2023 doi:10.20944/preprints202309.1107.v1

2.24 ± 0.31Hz; 5-HT, 3.18 ± 0.40Hz; p = 0.0046, based on a t-test) and shortened the time interval between events (Figure 2D: 10 cells; Control, 643.69 ± 200.26 ms; 5-HT, 367.94 ± 52.11 ms; p = 0.0078, based on a Wilcoxon signed-rank test).

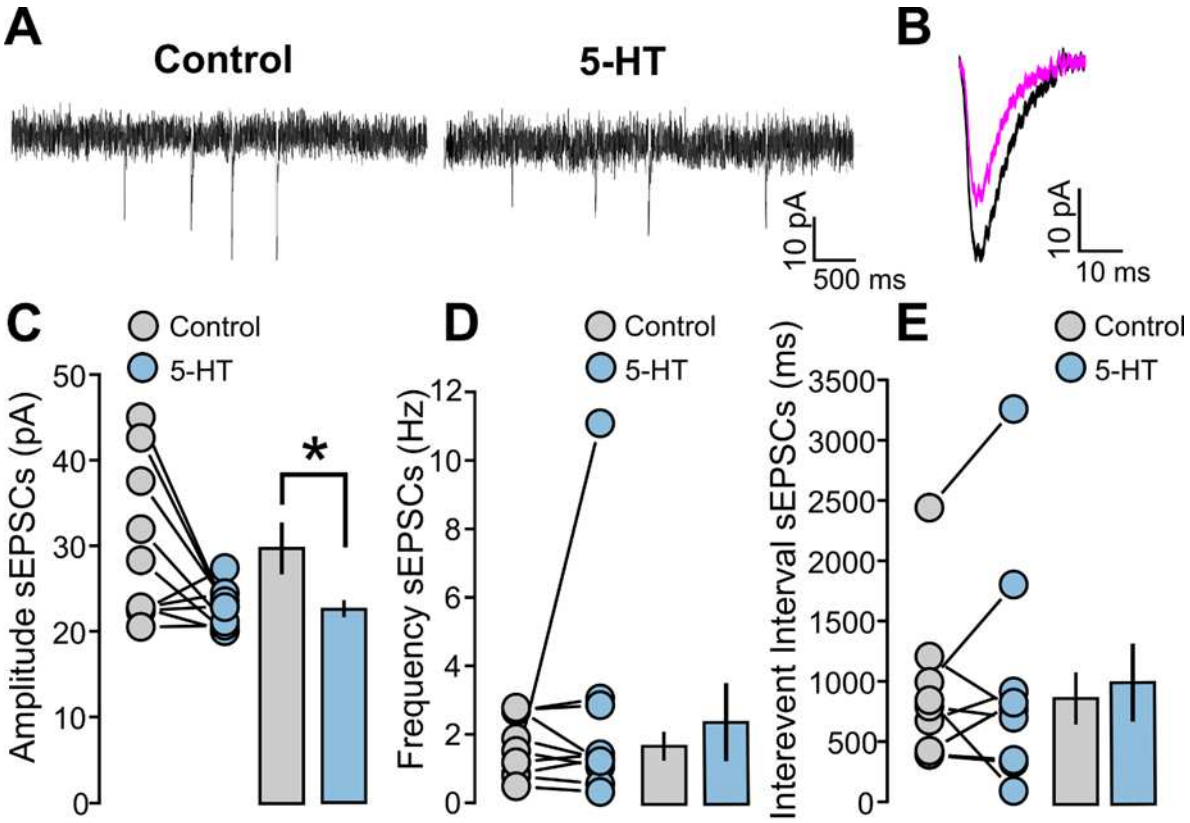

Figure 1. 5-HT decreases the amplitude of spontaneous excitatory synaptic currents (sEPSCs). **A**: Recorded example traces of the sEPSCs for the two conditions: 5-HT (50 μM) and control **B**: Average of the sEPSCs traces for the two conditions: 5-HT (50 μM) and control for one representative experiment **C**: The graph shows the data points and mean values of the sEPSCs amplitude (pA) for the two conditions: 5-HT (50 μM) and control. **D**: The graph shows the data points and mean values of the sEPSCs frequency (Hz) for the two conditions: 5-HT (50 μM) and control. **E**: The graph shows the data points and mean values of the sEPSCs interevent interval (ms) for the two conditions: 5-HT (50 μM) and control.

Preprints (www.preprints.org) | NOT PEER-REVIEWED | Posted: 18 September 2023 doi:10.20944/preprints202309.1107.v1

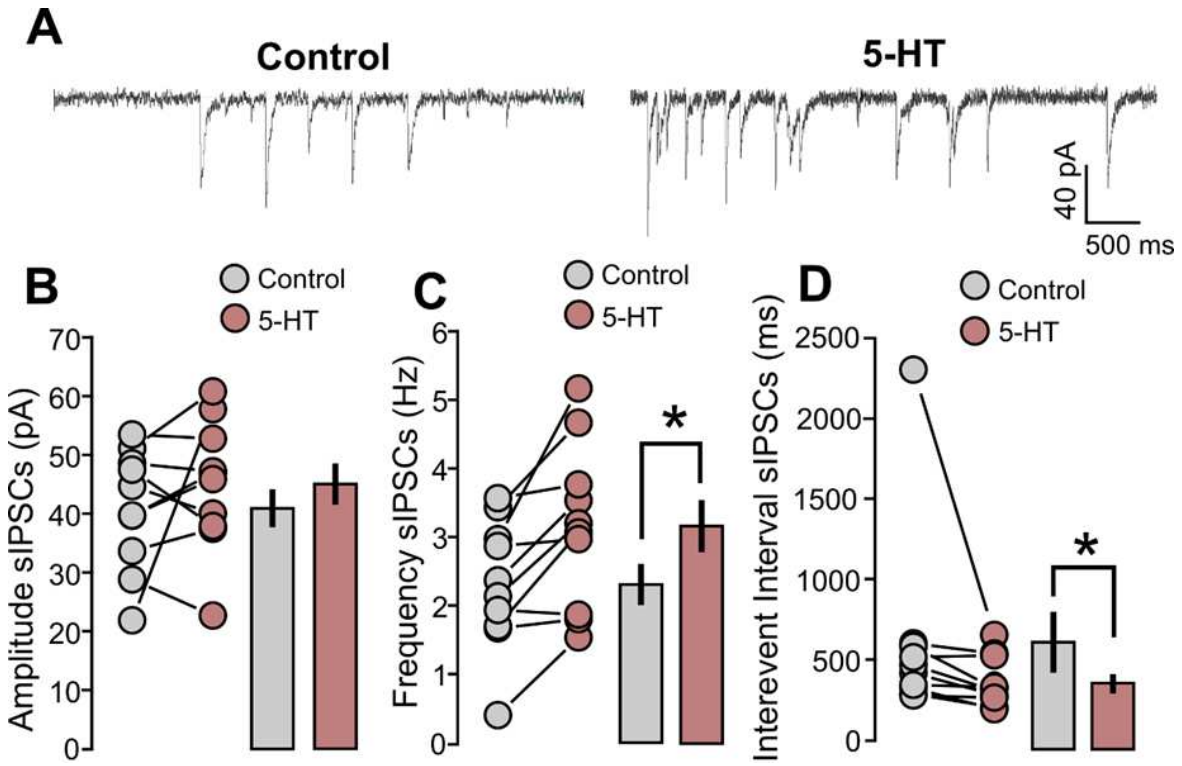

Figure 2. 5-HT increases the frequencies and decreases the interevent interval of spontaneous inhibitory synaptic currents (sIPSCs). **A**: Recorded example traces of the sIPSCs for the two conditions: 5-HT (50 μM) and control **B**: The graph shows the data points and mean values of the sIPSCs amplitude (pA) for the two conditions: 5-HT (50 μM) and control. **C**: The graph shows the data points and mean values of the sIPSCs frequency (Hz) for the two conditions: 5-HT (50 μM) and control. **D**: The graph shows the data points and mean values of the sIPSCs interevent interval (ms) for the two conditions: 5-HT (50 μM) and control. .

These results indicate that 5-HT modifies spontaneous synaptic activity by shifting the E/I ratio towards inhibition. Specifically, the 5-HT reduces the amplitude of glutamatergic currents while it increases the frequency of GABAergic postsynaptic responses.

2.2. Serotonin decreases excitatory and inhibitory evoked synaptic responses

The onset of visual experience and the sharpening of receptive field tuning properties requires a critical refinement of the input from layer 4 to layer 2/3 (layer 4-2/3) of V1[31, 35, 36]. Serotonergic modulation plays an important role in modulating this process during postnatal cortical development [37]. Based on this evidence, we focused our investigation on evoked excitatory postsynaptic potentials (eEPSPs) of layer 2/3 neurons obtained through stimulation of layer 4. After recording a 5 minutes baseline, we applied 5-HT (50 μM) in the bath for 15 minutes. We found that 5-HT significant reduces EPSPs by 20% (Figure 3A-B: 10 cells; 5-HT, 71.13 ± 8.18 % of baseline; $p = 0.0024$, based on a paired t-test).

5-HT signaling can affect the intrinsic excitability of cortical neurons by altering their membrane potential and input resistance [38, 39]. Therefore, it is possible that the reduction of synaptic transmission caused by 5-HT partially depends on changes in postsynaptic excitability. To test this possibility, we analyzed changes in the intrinsic membrane properties in those cells that were recorded for the evaluation of eEPSPs. We found that 5-HT did not cause any significant change in the membrane potential (Figure 3C-D: 12 cells; Control, -74.58 ± 1.94 mV; 5-HT, -76.548 ± 2.71 mV; $p = 0.4635$, based on a paired t-test) nor in the input resistance values (Figure 3E-F: 11 cells; Control, 190.91 ± 12.78 MΩ; 5-HT, 191.08 ± 20.92 MΩ; $p = 0.9923$, based on a paired t-test).

Preprints (www.preprints.org) | NOT PEER-REVIEWED | Posted: 18 September 2023 doi:10.20944/preprints202309.1107.v1

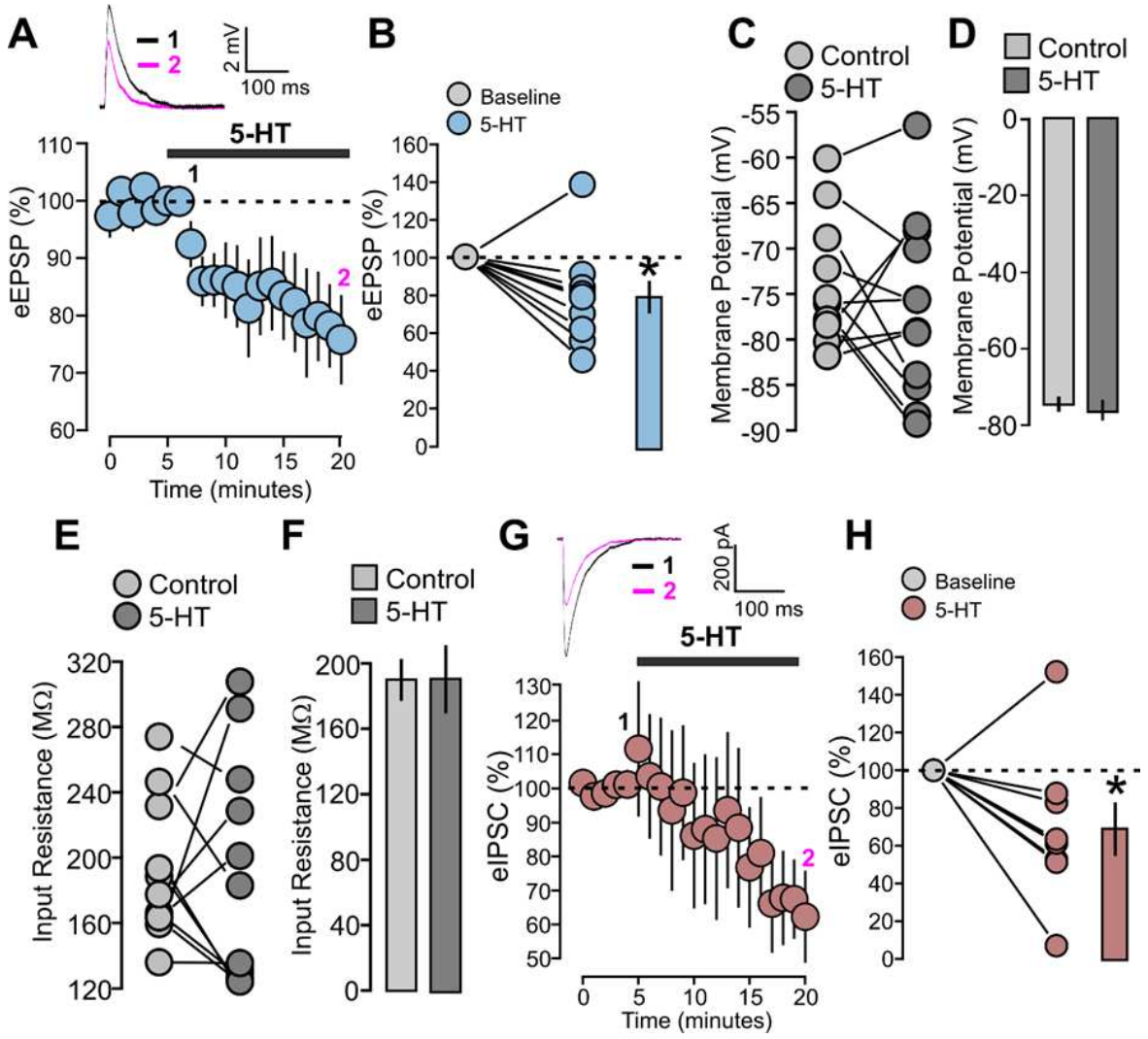

Figure 3. 5-HT decreases the evoked excitatory postsynaptic potentials (eEPSPs) and the evoked inhibitory postsynaptic currents (eIPSCs). **A**: The graph shows the eEPSPs recorded before and during 5-HT (50 μM) bath application. The EPSPs are normalized to the mean of responses recorded during the control baseline. Traces are showing one example experiment with the average of postsynaptic responses recorded before (Control; 1: 0 to 5 min, black line) and after (5-HT; 2: 15 to 20 min, magenta line) the application of 5-HT. **B**: The graph shows the data points and mean values of the normalized eEPSPs for the two conditions: 5-HT (50 μM) and control. **C**: The graph shows the data points of the membrane potential (mV) for the two conditions: 5-HT (50 μM) and control. **D**: The graph shows mean value of the membrane potential (mV) for the two conditions: 5-HT (50 μM) and control. **E**: The graph shows the data points of the input resistance (MΩ) for the two conditions: 5-HT (50 μM) and control. **F**: The graph shows mean value of the input resistance (MΩ) for the two conditions: 5-HT (50 μM) and control. **G**: The graph demonstrates the eIPSCs recorded before and during 5-HT (50 μM) bath application. The eIPSCs are normalized to the mean of responses recorded during the control baseline. Traces are showing one example experiment with the average of postsynaptic responses recorded before (Control; 1: 0 to 5 min, black line) and after (5-HT; 2: 15 to 20 min, magenta line) the application of 5-HT. **H**: The graph shows the data points and mean values of the normalized eIPSCs for the two conditions: 5-HT (50 μM) and control.

The strong feedforward layer 4-2/3 input is accompanied by the inhibitory activity of layer 4 interneurons, whose synapses can be modulated by 5-HT [40-43]. To study the effects of 5-HT on the GABAergic layer 4-2/3 input, we recorded the evoked inhibitory postsynaptic currents (eIPSCs) that were obtained by stimulation of the underlying layer 4. We first recorded a 5-minute baseline and subsequently administered 5-HT (50 μM) for 15 minutes. We found that 5-HT reduced the amplitude

 doi:10.20944/preprints202309.1107.v1

of eIPSCs and this effect is statistically significant (Figure 3G-H: 5-HT, 9 cells, 68.92 ± 12.94 % of baseline; p = 0.0430, based on a paired t-test).

Taken together, our results obtained from evoked excitatory and inhibitory postsynaptic responses indicate that 5-HT reduces the overall neuronal activity of the layer 4-2/3, maintaining the balance between excitation and inhibition relatively stable.

2.3. Serotonergic modulation promotes LTD at excitatory synapses

In addition to acting directly on synaptic transmission, 5-HT may also regulate synaptic plasticity induced by specific patterns of paired pre- and postsynaptic activity [44-46]. The regulatory effects on plasticity provided by neuromodulators have been found to modulate electrically induced synaptic plasticity [47, 48]. In this regard, it has become known that neuromodulator-mediated synaptic plasticity is fundamental in promoting synaptic changes and defining their polarity in the visual cortical circuitry [8, 47-49].

Based on these observations and still focusing on the layer 4-2/3 synaptic transmission, we investigated the modulatory effects of 5-HT on the expression of LTD induced through a paired protocol, where postsynaptic firing was induced 10 milliseconds prior to presynaptic stimulation. Graphs A and B of Figure 4 show the eEPSPs recorded in the control condition without the presence of 5-HT. After a 10-minute baseline, the paired protocol was applied and the eEPSPs were recorded over a 40-minute period. No significant difference in the mean amplitude of eEPSPs was found when comparing the baseline with the last 5 minutes of the post-induction period (Figure 4A-B: Control, 11 cells, 89.43 ± 17.06% of baseline; p = 0.5693, based on a paired t-test). We then adopted the same paired protocol in cells incubated with 5-HT (50 μM) for 20 minutes and kept in the presence of the neuromodulator in the bath throughout the whole duration of the experiment. Under this condition, the paired protocol caused a significant depression of eEPSPs (Figure 4C-D: 5-HT, 9 cells, 50.41 ± 10.68 % of baseline; p = 0.0017, based on a paired t-test).

These results indicate that the expression of LTD is facilitated by the presence of 5-HT. This is consistent with the general view of neuromodulators' effects on plasticity, according to which their action is a critical factor that facilitates modification of synaptic strength in visual cortical circuits [47, 48].

Preprints (www.preprints.org) | NOT PEER-REVIEWED | Posted: 18 September 2023 doi:10.20944/preprints202309.1107.v1

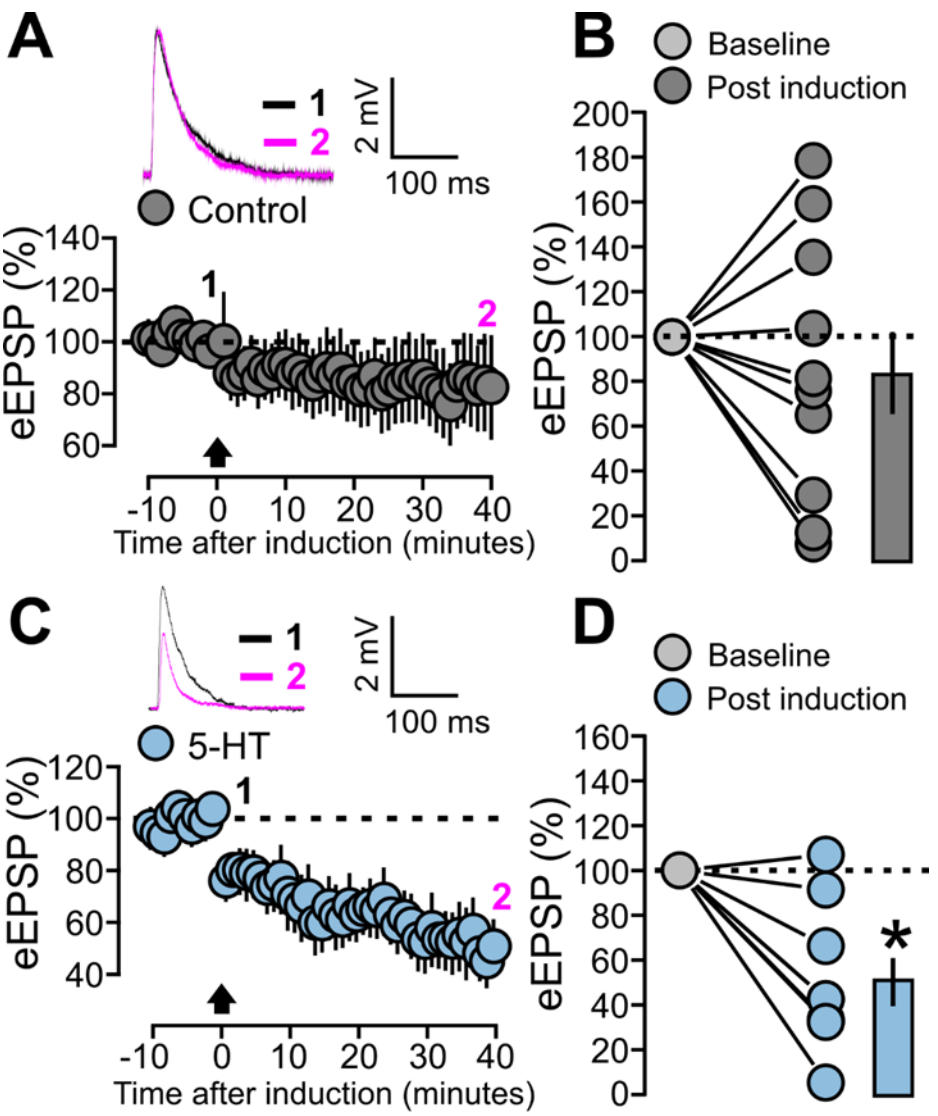

Figure 4. 5-HT promotes the LTD at excitatory synapses (eLTD). A: The graph shows the eEPSPs recorded before and after the paired protocol induction in the control condition (without bath application of 5-HT). The eEPSPs are normalized to the mean of responses recorded during the last 5 minutes of the baseline. Traces are showing one example experiment with the average of postsynaptic responses recorded before (Baseline; 1: 5 to 10 min, black line) and after (Post induction; 2: 35 to 40 min, magenta line) the application of the paired protocol. B: The graph shows the effects of the paired protocol on eEPSPs in the control condition (without bath application of 5-HT). The data points and mean values of the normalized eEPSPs are shown for the two conditions: baseline and post induction. C: The graph shows the eEPSPs recorded before and after the paired protocol induction during bath application of 5-HT (50 μM). The eEPSPs are normalized to the mean of responses recorded during the last 5 minutes of the baseline. Traces are showing one example experiment with the average of postsynaptic responses recorded before (Baseline; 1: 5 to 10 min, black line) and after (Post induction; 2: 35 to 40 min, magenta line) the application of the paired protocol. D: The graph shows the effects of the paired protocol on eEPSPs during bath application of 5-HT (50 μM). The data points and mean values of the normalized eEPSPs are shown for the two conditions: baseline and post induction.

2.4. Serotonin decreases neuronal spiking and increases the action potential amplitude

During the paired protocol application, the back-propagating of action potential depolarizes dendritic postsynaptic sites as a step of the induction [50, 51]. This implies that the outcome of synaptic change depends on the spiking pattern and action potential properties of postsynaptic neurons [52, 53]. The intracellular signaling activated by neuromodulators can modify the neuronal spiking activity,

Preprints (www.preprints.org) | NOT PEER-REVIEWED | Posted: 18 September 2023 doi:10.20944/preprints202309.1107.v1

and these effects may influence the expression of synaptic modification [54]. These insights suggest the possibility that 5-HT may affect the plasticity outcome by altering the spiking properties of the postsynaptic neuron. To test this hypothesis, we studied the effects of 5-HT (50 μM) on the spiking activity of layer 2/3 neurons, by comparing two experimental groups. The first group consisted of brain slices incubated with 5-HT-treated ACSF for 20 minutes. The second group consisted of control brain slices that were not treated with the neuromodulator. The spiking activity was then studied by subjecting the cells to progressive injection steps of depolarizing current from 40 pA to 200 pA.

As shown in Figure 5, cells treated with 5-HT exhibited significantly fewer action potentials in response to excitatory currents for the 80 pA current step (Figure 5A-B: 80 pA; Control, 29 cells, 0.69 ± 0.19; 5-HT, 17 cells, 0.18 ± 0.13; p = 0.0419, based on a Mann Whitney U test), for the 120 pA current step (Figure 5A-B: 120 pA; Control, 29 cells, 2.28 ± 0.35; 5-HT, 17 cells, 0.94 ± 0.33; p = 0.0189, based on a Mann Whitney U test) and for the 160 pA current step (Figure 5A-B: 160 pA; Control, 29 cells, 3.69 ± 0.39; 5-HT, 17 cells, 2.35 ± 0.41; p = 0.0321, based on a unpaired t-test). We also found that cells treated with 5-HT had a higher rheobase, i.e., the minimum current step that causes action potential firing (Figure 5C-D: Control, 29 cells, 114.48 ± 7.62; 5-HT, 17 cells, 145.88 ± 10.26; p = 0.0204, based on a Mann Whitney U test).

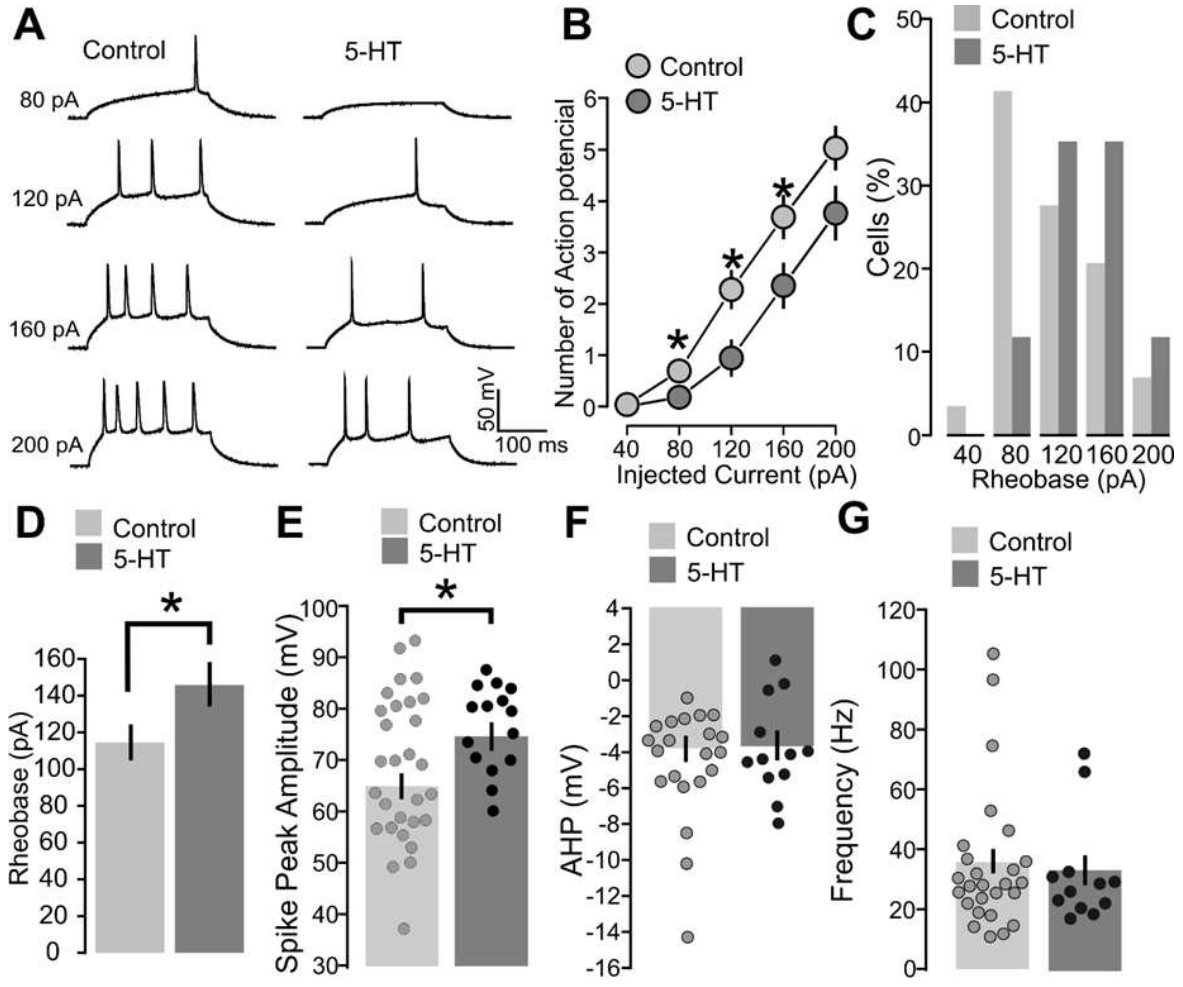

Figure 5. 5-HT increases the rheobase for neuronal spiking and the action potential peak amplitude. **A**: Recorded example traces of the action potential firing for the two conditions: 5-HT (50 μM) and control. The spiking response is shown for 80, 120, 160 and 200 pA. **B**: The graph shows the average of the mean number of action potentials fired for the two conditions: 5-HT (50 μM) and control. The number of action potential is plotted against the value of the injected current step (pA) **C**: The graph shows the distribution of rheobase values among the population of recorded cells. The current values of all injected current steps (80, 120, 160 and 200 pA) are plotted against the percentage of cells. **D**: The graph shows the mean values of the rheobase values (pA) for the two conditions: 5-HT (50 μM) and control. **E**: The graph shows the data points and mean values of the spike peak amplitude (mV)

 doi:10.20944/preprints202309.1107.v1

for the two conditions: 5-HT (50 μM) and control. **F**: The graph shows the data points and mean values of the after hyperpolarizationClique aqui para inserir texto. (mV) for the two conditions: 5-HT (50 μM) and control. **G**: The graph shows the data points and mean values of the spiking frequency (Hz) for the two conditions: 5-HT (50 μM) and control.

We next analyzed the traces of cells stimulated with the 200 pA current pulse and quantified the action potentials properties: the peak amplitude, the after-hyperpolarization (AHP) amplitude, and the firing frequency We found that neurons treated with 5-HT exhibited higher action potential peak amplitude (Figure 5E: Control, 27 cells, 64.87 ± 2.54; 5-HT, 12 cells, 74.37 ± 2.42; p = 0.0114, based on a unpaired t-test). On the other hand, no difference was observed in terms of AHP amplitude (Figure 5F: Control, 25 cells, -3.79 ± 0.72; 5-HT, 12 cells, -3.71± 0.79; p = 0.9430, based on a t-test) and firing frequency (Figure 5G: Control, 26 cells, 35.18 ± 4.66; 5-HT, 11 cells, 35.18 ± 5.40; p = 0.2248, based on a Mann Whitney U test).

These results show that 5-HT reduces neuronal excitability since its presence increases the current required to achieve firing and reduces the number of evoked spikes. However, the neuromodulator increases the amplitude of the depolarizing peak of the action potential. This process could possibly result in higher back-propagating excitation and facilitation of synaptic plasticity.

2.5. Serotonin blocks the LTD at inhibitory synapses

Electrophysiological studies in the early 1990s demonstrated that sustained depolarization of pyramidal neurons leads to depression of inhibitory synaptic inputs by decreasing the amount of GABA released from the interneuron´s synapses [55, 56]. Later on, other studies found that theta burst stimulation applied at excitatory synapses of superficial layers in the visual cortex elicit the reduction of inhibitory synaptic currents [57, 58]. These works suggest the existence of a heterosynaptic interaction between excitatory and inhibitory synapses in pyramidal neurons. According to this perspective, the induction of plasticity at the glutamatergic pathway can activate extracellular messengers, which in turns can modify the strength of neighboring GABAergic connections.

We then performed the same experiment under the effects of 5-HT (50 μM). Though, the paired protocol did not cause significant alteration of eIPSCs with respect to the baseline (Figure 6C-D: 5-HT, 9 cells, 144.68 ± 33.51 % of baseline; p = 0.3008, based on a Wilcoxon signed-rank test). These results indicate that the paired protocol at the layer 4-2/3 input causes LTD at inhibitory connections and this process can be blocked by 5-HT.

To investigate this possibility, we designed a set of experiments aimed to verify whether the paired protocol causes synaptic alterations at inhibitory synapses and whether this process can be modulated by 5-HT. In these experiments, the evoked postsynaptic inhibitory currents (eIPSCs) of the layer 4-2/3 input were recorded in the voltage-clamp mode, with +10 mV holding potential. After establishing a 10-minute baseline, the recording was switched to current-clamp mode for the induction of the paired protocol. Our results show that the paired protocol resulted in a significant LTD of the eIPSCs (Figure 6A-B: Control, 10 cells, 62.92 ± 9.66 % of baseline; p = 0.0066, based on a paired t-test).

Preprints (www.preprints.org) | NOT PEER-REVIEWED | Posted: 18 September 2023 doi:10.20944/preprints202309.1107.v1

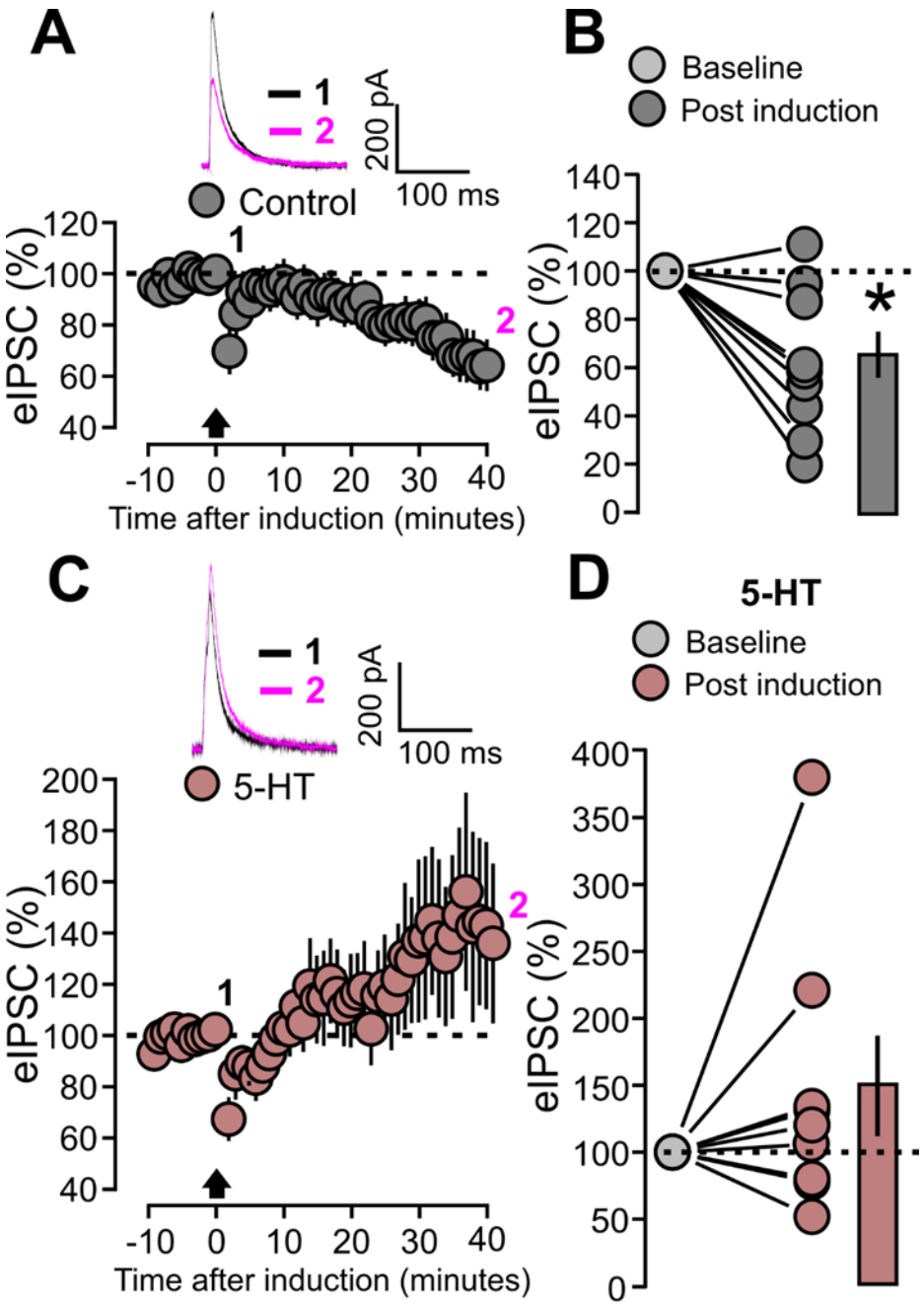

Figure 6. 5-HT prevents the LTD at inhibitory synapses (iLTD). **A**: The graph shows the eIPSCs recorded before and after the paired protocol induction in the control condition (without bath application of 5-HT). The eIPSCs are normalized to the mean of responses recorded during the last 5 minutes of the baseline. Traces are showing one example experiment with the average of postsynaptic responses recorded before (Baseline; 1: 5 to 10 min, black line) and after (Post induction; 2: 35 to 40 min, magenta line) the application of the paired protocol. **B**: The graph shows the effects of the paired protocol on eIPSCs in the control condition (without bath application of 5-HT). The data points and mean values of the normalized eIPSCs are shown for the two conditions: baseline and post induction. **C**: The graph shows the eIPSCs recorded before and after the paired protocol induction during bath application of 5-HT (50 μM). The eIPSCs are normalized to the mean of responses recorded during the last 5 minutes of the baseline. Traces are showing one example experiment with the average of postsynaptic responses recorded before (Baseline; 1: 5 to 10 min, black line) and after (Post induction; 2: 35 to 40 min, magenta line) the application of the paired protocol. **D**: The graph shows the effects of the paired protocol on eIPSCs during bath application of 5-HT (50 μM). The data points and mean values of the normalized eIPSCs are shown for the two conditions: baseline and post induction.

 doi:10.20944/preprints202309.1107.v1

3. DISCUSSION

The present study investigated serotonergic modulation of the E/I balance in layer 2/3 of mice V1, during the critical period of synaptic plasticity. We found that 5-HT decreases the amplitude of spontaneous excitatory inputs, while increases the frequency of spontaneous inhibitory currents. Focusing on the evoked signals at the pathway from layer 4 to layer 2/3 (layer 4-2/3 input), 5-HT was found to decrease both excitatory and inhibitory synaptic responses. Finally, we show that 5-HT facilitates LTD at excitatory synapses (eLTD) of the layer 4-2/3 pathway and prevents the depression of inhibitory synapses (iLTD) instead.

Our data from spontaneous activity experiments suggest that 5-HT decreases the E/I balance of developing V1. This is in agreement with previous studies. 5-HT was found to suppress glutamatergic synaptic transmission by activation of synaptic 5-HT_{1A} and 5-HT_7 receptors in layer 2/3 pyramidal neurons, at early stages of postnatal development of rat V1[59]. Similarly, in the visual cortex of ferrets, 5-HT_3 receptors decrease the E/I balance throughout postnatal development by reducing excitatory synaptic responses and increasing spontaneous GABAergic synaptic currents [60]. Interestingly, in vivo studies indicate that 5-HT-mediated reduction of visual cortical excitation provides balanced effects on glutamatergic spontaneous activity across neuronal populations, which is functional to increase the visual response gain.[61-63] In our study, 5-HT increased the frequency of spontaneous inhibition but not its amplitude, suggesting that 5-HT had a limited effect on the action potential-evoked calcium influx. 5-HT signaling may instead affect GABA release at inhibitory terminals. This interpretation is consistent with other works showing that 5-HT_{2A} receptor stimulation leads to an increase of intracellular calcium concentration, which in turn might up-regulate the number of vesicles available for presynaptic release [64, 65].

We found an important discrepancy between the observed E/I balance from spontaneous currents and the comparison between evoked excitatory and inhibitory inputs in the layer 4-2/3 pathway. While spontaneous activity indicates a 5-HT-mediated reduction of the E/I balance, the neuromodulator does not seem to modify this ratio in the layer 4-2/3 input. This discrepancy probably arises from the fact that spontaneous neural activity in layer 2/3 includes many inhibitory signals that derive from interneurons located at superficial layers. Based on this perspective, it is possible to speculate that 5-HT might modulate the E/I balance of intralayer and interlayer neural activity in different ways and this difference would reflect important functional consequences.

Layer 4 interneurons provide superficial layers with fast and strong feedforward inhibition, which serves as a general gain control for the processing of visual inputs [66-68]. The strength of this inhibition is a key factor for the timing of neuronal processing, playing an important role in the selection of coincident sensory inputs and in the effective propagation of visual information [69]. On the other hand, intralaminar inhibition to layer 2/3 pyramidal cells operates in the process of shaping the receptive field properties [70-73]. This functional difference is particularly relevant when the visual cortex is activated by gamma rhythms (20–80 Hz), which require a dynamic relationship between excitation and inhibition [74-76]. Gamma activity depends on reciprocal interaction between recurrently connected excitation and inhibition, which is correlated with perception, attention, and cognition [74, 76, 77]. Recurrent inhibition of layer 2/3 allows neural activity to remain constant and synchronized through the visual cortical map [78-82]. Inputs from intralaminar GABAergic interneurons to pyramidal neurons contribute to a relatively low E/I balance that prevents the runaway of neural activity. On the other hand, excitation at layer 2/3 increases when the layer 4-2/3 input propagates neural information and promotes spiking at its downstream targets [76]. Combined with this model, our results suggest the hypothesis that 5-HT reduces the E/I balance of local intralaminar activity while affecting to a lesser extent the information relay across the interlaminar connections. Interestingly, such 5-HT effects on layer 4-2/3 pathway are different at older ages (P35), when the E/I balance is reduced due to increase of inhibitory postsynaptic currents [40]. Thus, the layer 4-2/3 input might maintain a relatively higher level of excitation only during postnatal development and this fact could partly explain a more inducible synaptic plasticity, which is typical of early ages [57, 83].

We show that 5-HT facilitates the LTD induced through a paired protocol in which presynaptic stimulation is preceded by neuronal firing. This finding is in agreement with previous studies, which

demonstrated that neuromodulators are a key factor for the expression and direction of synaptic changes induced through paired protocols in the developing visual cortex [8, 47, 48]. The capacity of 5-HT to promote plasticity in V1 during the critical period has first been observed in kittens, during the 1990s. Visual experience controlled the columnar specific organization of 5-HT_2 receptors and ocular dominance plasticity could be reduced with 5-HT_{2C} antagonists [4, 84]. In rodents, the action of 5-HT as a facilitator of plasticity has been mostly investigated in the mature brain. Increased levels of 5-HT in the V1 of adult rats restore LTP and ocular dominance plasticity [85-88]. These effects can be either achieved through the administration of fluoxetine (an antidepressant that increases serotonergic activity) or through a 5-HT-dependent mechanism elicited by environmental enrichment. However, the role of 5-HT as a neuromodulator of plasticity during the critical period is less clear. One previous study carried out in this direction found that 5-HT inhibits the TBS-induced LTP in V1 at P20-35 [89-91]. Our results pointed out the existence of an LTD during the critical period which is promoted by the presence of 5-HT. Taken together with previous studies, our findings suggest a complex age-dependent role of 5-HT. In the young V1, serotonergic modulation reduces LTP and favors LTD, while, in the adult brain, 5-HT could be more active in promoting synaptic reinforcement processes.

The study of the firing properties of pyramidal neurons in layer 2/3 showed that 5-HT increases the minimal current required for action potential elicitation, indicating a reduction in excitability that has already been observed in other cortical neurons [38, 92, 93]. However, we found that the spike amplitude is increased with the presence of 5-HT. The amplitude of back-propagating action potentials influences the plasticity outcome of spike-timing dependent plasticity [52, 53]. 5-HT may facilitate LTD induction in part by providing increased back-propagating excitation, thus providing longer-lasting depolarization at activated synaptic sites.

Our data obtained from inhibitory current recordings show that the paired protocols resulted in the iLTD at GABAergic terminals. This phenomenon could depend on the heterosynaptic retrograde signaling mediated by endocannabinoids, according to a process that has been defined as the reduction of inhibition induced by local excitation [94, 95]. This form of heterosynaptic interaction has also been observed in V1 plasticity at early ages, where TBS-induced LTP relies on the concomitant expression of iLTD and this process has been associated to the maturation of cortical GABAergic inhibition [57, 58].

In our study, the paired induction failed to cause significant depression at the glutamatergic sites but was effective for the induction of iLTD. Considering the Hebbian rule as applied to heterosynaptic mechanisms of competition, it has been suggested that the endocannabinoids-mediated iLTD may facilitate plasticity occurring at synapses elected for enhancement [96]. The presence of 5-HT, however, seems to reverse this condition. By promoting eLTD at the stimulated excitatory synapses and by blocking the iLTD at GABAergic terminals, the neuromodulator appears to shift the Hebbian dispute to lower levels of the E/I balance. This idea is supported by the evidence that 5-HT inhibits LTP at P21-35, through the up-regulation of $GABA_A$ receptors activity [89].

4. MATERIALS AND METHODS

4.1. Animals

All procedures carried out in this project were approved by the Institutional Animal Care Committee of the Institute of Biomedical Sciences (ICB), University of São Paulo, Brazil (CEUA/ICB/USP; #1336091118). C57BL/6 mice of either sex at the age of postnatal day 21-24 (P21-24) were used. The animals were kept in their respective litters in the animal facility of the Department of Physiology and Biophysics at ICB/USP under standard conditions: 23 ± 2 °C, 12 h light/dark cycle, light-dark cycle of 12: 12 hours (lights on 6h00 a.m.), food and water ad libitum, lighting ~ 200 lx.

4.2. Preparation and maintenance of slices

The animals were anesthetized with isoflurane inhalation (5% isoflurane in oxygen) and then decapitated. The brain was quickly removed and transferred to a buffer solution (ice cold) composed of (in mM): 212.7 sucrose, 5 KCl, 1.25 NaH_2PO_4, 10 $MgCl_2$, 0.5 $CaCl_2$, 26 $NaHCO_3$, 10 dextrose; in the

presence of carbogen (95% O_2 - 5% CO_2), pH 7.4. Once in solution, coronal slices of visual cortex (300-350 μm) were cut using a vibratome (VT 1200-S, Leica Biosystems). Slices were quickly transferred in an artificial cerebrospinal fluid solution: ACSF; composition (in mM): 124 NaCl, 5 KCl, 1.25 NaH_2PO_4, 1 $MgCl_2$, 2 $CaCl_2$, 26 $NaHCO_3$, 10 dextrose, in the presence of carbogen (95% O_2/5% CO_2) at pH 7.3-7.4. Slices were kept oxygenated at room temperature (RT, 20–25 °C) for 1 h before electrophysiological experiments.

4.3. Electrophysiological recordings

The slices were placed in a perfusion chamber attached to the microscope (Eclipse E600FN, Nikon) and were subjected to perfusion of ACSF solution (1.5 mL/min). Recording electrodes pipettes were fabricated from borosilicate glass (Garner Glass; California, USA) with input resistances of ~4–6 MΩ and were filled with intracellular solution. Two kinds of intracellular solution were used: a K-Gluconate solution and a Cs-Cl solution. The K-Gluconate solution had the following composition (in mM): 130 K-Gluconate, 10 KCl, 0.2 EGTA, 10 HEPES, 4 MgATP, 0.5 NaGTP, 10 Na-Phosphocreatine. The pH was adjusted to 7.3 with KOH and the osmolarity was adjusted to 290 mOsm. The Cs-Cl solution had the following composition (in mM): 30 CsCl, 10 HEPES, 5 EGTA, 5 Na-Phosphocreatine, 4 MgATP, 0.5 NaGTP, 10 TEA, 5 QX-314. The pH was adjusted to 7.3 with CsOH and the osmolarity was adjusted to 290 mOsm.

Intracellular recordings were performed from layer 2/3 regular spiking pyramidal neurons of the primary visual cortex in the *whole-cell* modality of patch-clamp. Pyramidal-shaped cells were visualized and selected by means of a fixed-base microscope (Eclipse E600FN; Nikon) through a 40X objective (CFI Apochromat NIR 40X W, NA: 0.80, W.D.: 3.5) and an electronic micromanipulator (MPC-385 System; Sutter Instrument Company, USA) was used to approach the recorded cell. All recordings were filtered at 2 kHz and digitized at 5 kHz using a Digidata 1332 digitizing board (Axon, Molecular Devices, USA) connected to a Multiclamp700B amplifier (Axon, Molecular Devices, USA). We only included in our data cells with membrane potential lower than -60 mV, with input resistance varying between 100 and 1000 MΩ and with access resistance lower than 20 MΩ (with compensation of 80%). For all experimental groups, no more than two cells were recorded from the same animal.

4.4. Spontaneous postsynaptic currents

The recording of spontaneous postsynaptic responses was performed with the *Cs-Cl* intracellular solution, in voltage-clamp mode with a holding potential of -70 mV. The basal activity of spontaneous postsynaptic currents was recorded for a 10 minutes period, after which 5-HT (50 μM) was added to the bath for 10 minutes. The analysis was performed by comparing the last 30 seconds of the basal activity with the last 30 seconds of the recording with the presence of 5-HT.

The isolation of spontaneous excitatory postsynaptic currents (sEPSCs) was achieved by applying the $GABA_A$ receptor antagonist Picrotoxin (50 μM; Tocris: Cat. No. 1128) in the ACSF to block the currents through GABAergic ionotropic receptors.. Recording of spontaneous inhibitory postsynaptic (sIPSCs) adopted the ionotropic glutamatergic antagonist DNQX (50 μM; Tocris: Cat. No. 0189) in the ACSF to block the currents through AMPA receptors. To block NMDA receptor currents, the antagonist MK-801 (50 μM, Tocris, Cat. No. 0924) was used.

4.5. Neuronal firing

In experiments where the effects of 5-HT on action potential (AP) firing were investigated, electrical features under current injection in pyramidal neurons from layer 2/3 were extracted using the Electrophys Feature Extraction Library (eFEL) [https://github.com/BlueBrain/eFEL]. Neurons were depolarized with 250 ms current steps (40, 80, 120, 160, and 200 pA). The rheobase was defined as the minimum current step which elicits AP firing. The 200 pA step was used to analyze the AP peak amplitude the after hyperpolarization (AHP) amplitude and the mean firing frequency. The AP peak the after hyperpolarization (AHP) amplitudes were calculated as the relative maximum and minimum voltage value, respectively, with respect to the onset of the AP, by averaging the values of

 doi:10.20944/preprints202309.1107.v1

the first 3 AP. The mean frequency was calculated by averaging the frequency values obtained from the two first interevent intervals.

4.6. Evoked postsynaptic responses and stimulation

Evoked excitatory postsynaptic potentials (eEPSPs) or evoked inhibitory postsynaptic currents (eIPSCs) were recorded by electrically stimulating the inputs from layer 4 to pyramidal neurons of layer 2/3 (0.2 ms). A concentric bipolar electrode (125 μm diameter) was placed on layer 4 and the intensity of stimulation was increased gradually by steps of 5 μA from a sub-threshold level until a response was evoked.

4.7. Serotonergic modulation of evoked postsynaptic responses

In experiments aimed to study serotonergic modulation of evoked synaptic inputs, synaptic responses were evoked every 10 seconds. 5-HT (50 μM) was added to the bath after 5 minutes of stable recording (baseline), and synaptic responses were further recorded for 15 minutes, under the effects of 5-HT. Data were discarded if the access resistance or input resistance changed > 20% during the baseline recording. Changes of input resistance and membrane caused by 5-HT were quantified and analyzed by calculating the average values of the last 5 min of the baseline and by comparing these values with the average values of the last 5 min of 5-HT recordings.

Glutamatergic evoked postsynaptic potentials (eEPSPs) were recorded with the K-Gluconate intracellular solution in current clamp mode at free membrane potential (I = 0). Evoked GABAergic responses (eIPSCs) were recorded in voltage-clamp mode, with the Cs-Cl intracellular solution, holding at -70 mV. When studying the 5-HT effects on eIPSCs, DNQX (50 μM; Tocris: Cat. No. 0189) and MK-801 (50 μM, Tocris, Cat. No. 0924) were used to block the AMPA and NMDA receptors respectively. Both EPSPs and IPSCs were normalized to the averaged responses value of the 5 minutes baseline. Changes in synaptic strength caused by 5-HT were quantified as changes in the initial amplitude of the postsynaptic potential normalized by the mean response obtained during the last 5 minutes of recording.

4.8. Serotonergic modulation of synaptic plasticity

In experiments where synaptic plasticity was investigated, the effects of the same paired protocol was applied either for the study of excitatory synapses (eLTD) or for the study of inhibitory synapses (iLTD). When eLTD was evaluated, excitatory postsynaptic potentials (EPSPs) were recorded in current-clamp mode (I=0) with the K-Gluconate intracellular solution. When iLTD was assessed, inhibitory postsynaptic currents (IPSCs) were recorded in voltage-clamp mode with a +10 mV holding potential and K-Gluconate intracellular solution. The induction of the paired protocol was achieved by applying 200 pairing epochs at 1 Hz. The pairing epoch consisted in four action potentials (100 Hz) evoked by passing 1.5 threshold depolarizing current steps through the recording electrode (~1 nA, 2 ms), 10 milliseconds prior to a presynaptic stimulation pulse (0.2 ms).

For both eLTD and iLTD experiments, two experimental groups were adopted: 5-HT and control slices. Slices from the 5-HT group were incubated with 5-HT (50 μM) for 20 minutes. Subsequently, the slices were introduced to the synaptic plasticity experiment and 5-HT was maintained at the same concentration during the whole experiment. Control slices were treated in the same conditions, but without 5-HT. Synaptic responses were evoked every 10 seconds by stimulating layer 4 with 0.2 ms pulses. The paired protocol was delivered after 10 minutes of stable recording (baseline) and data were discarded if the access resistance or input resistance changed > 20% during the baseline recording. After the plasticity induction, synaptic responses were further recorded for 40 minutes. Changes in EPSPs or IPSCs were normalized to the last 5 minutes of the baseline, and synaptic change induced by the paired protocol was quantified by calculating the normalized amplitude average of the last 5 min (35–40 min) and by comparing this value with the normalized amplitude average of the last 5 min of the baseline (5–10 min).

4.10. Statistical methods

For all data, normality was tested by means of the Shapiro–Wilk test. In experiments where data were normally distributed, statistical analysis was performed by using parametric tests. When the experimental groups were two paired samples, the paired t-test was used. When the experimental groups were not paired samples, the unpaired t-test was used. In experiments where data were not normally distributed and the mean differences between groups were split on one variable, statistical analysis was performed by using non-parametric tests. When the experimental groups where paired samples, the Wilcoxon signed-rank test was used. When the experimental groups where two independent samples, the Mann–Whitney U test was used. All experimental groups were considered significantly different for p values lower than 0.05.

Author Contributions: Conceptualization, Estevão Carlos-Lima and Roberto De Pasquale; Data curation, Estevão Carlos-Lima, Guilherme Shigueto Vilar Higa and Roberto De Pasquale; Formal analysis, Estevão Carlos-Lima, Fernando da Silva Borges and Roberto De Pasquale; Investigation, Estevão Carlos-Lima, Guilherme Shigueto Vilar Higa, Felipe José Costa Viana, Alicia Moraes Tamais and José Francis-Oliveira; Methodology, Estevão Carlos-Lima, Guilherme Shigueto Vilar Higa and Roberto De Pasquale; Resources, Roberto De Pasquale; Software, Fernando da Silva Borges; Supervision, Roberto De Pasquale; Validation, Roberto De Pasquale; Visualization, Roberto De Pasquale; Writing – original draft, Guilherme Shigueto Vilar Higa and Roberto De Pasquale; Writing – review & editing, Guilherme Shigueto Vilar Higa and Roberto De Pasquale.

Informed Consent Statement: all procedures carried out in this project were approved by the Institutional Animal Care Committee of the Institute of Biomedical Sciences (ICB), University of São Paulo, Brazil (CEUA/ICB/ USP; #1336091118).

Data Availability Statement: the data that support the findings of this study are available from Roberto De Pasquale, but restrictions apply to the availability of these data, which were used under license for the current study, and so are not publicly available. Data are however available from the authors upon reasonable request and with permission of Roberto De Pasquale.

Acknowledgments: This work was supported by São Paulo Research Foundation (FAPESP): grant numbers 2022/00850-3, 2019/14962-5 and 2019/21233-0. It was also supported by the Coordenação de Aperfeiçoamento de Pessoal de Nível Superior (CAPES) and the Conselho Nacional de Pesquisas (CNPq; 140361/2020-0), Edital de Apoio a Projetos Integrados de Pesquisa em Áreas Estratégicas (PIPAE) of Research Support Center of the University of São Paulo – Process USP no: 2021.1.10424.1.9.

Conflicts of Interest statement: The authors declare no conflict of interests.

References

1. Baumgarten HG, Grozdanovic Z. Psychopharmacology of central serotonergic systems. Pharmacopsychiatry 1995;28 Suppl 2:73-79.
2. Jacobs BL, Azmitia EC. Structure and function of the brain serotonin system. Physiol Rev 1992;72:165-229.
3. Bunin MA, Wightman RM. Paracrine neurotransmission in the CNS: involvement of 5-HT. Trends Neurosci 1999;22:377-382.
4. Gu Q, Singer W. Involvement of serotonin in developmental plasticity of kitten visual cortex. Eur J Neurosci 1995;7:1146-1153.
5. Pazos A, Cortés R, Palacios JM. Quantitative autoradiographic mapping of serotonin receptors in the rat brain. II. Serotonin-2 receptors. Brain Res 1985;346:231-249.
6. Pazos A, Palacios JM. Quantitative autoradiographic mapping of serotonin receptors in the rat brain. I. Serotonin-1 receptors. Brain Res 1985;346:205-230.
7. Pompeiano M, Palacios JM, Mengod G. Distribution and cellular localization of mRNA coding for 5-HT1A receptor in the rat brain: correlation with receptor binding. J Neurosci 1992;12:440-453.
8. Hong SZ, Mesik L, Grossman CD, et al. Norepinephrine potentiates and serotonin depresses visual cortical responses by transforming eligibility traces. Nat Commun 2022;13:3202.
9. Frémaux N, Sprekeler H, Gerstner W. Reinforcement learning using a continuous time actor-critic framework with spiking neurons. PLoS Comput Biol 2013;9:e1003024.

10. Zuo W, Zhang Y, Xie G, Gregor D, Bekker A, Ye JH. Serotonin stimulates lateral habenula via activation of the post-synaptic serotonin 2/3 receptors and transient receptor potential channels. Neuropharmacology 2016;101:449-459.
11. Gaspar P, Cases O, Maroteaux L. The developmental role of serotonin: news from mouse molecular genetics. Nat Rev Neurosci 2003;4:1002-1012.
12. Pascucci T, Andolina D, Ventura R, Puglisi-Allegra S, Cabib S. Reduced availability of brain amines during critical phases of postnatal development in a genetic mouse model of cognitive delay. Brain Res 2008;1217:232-238.
13. Rebello TJ, Yu Q, Goodfellow NM, et al. Postnatal day 2 to 11 constitutes a 5-HT-sensitive period impacting adult mPFC function. J Neurosci 2014;34:12379-12393.
14. Vinkers CH, Oosting RS, van Bogaert MJ, Olivier B, Groenink L. Early-life blockade of 5-HT(1A) receptors alters adult anxiety behavior and benzodiazepine sensitivity. Biol Psychiatry 2010;67:309-316.
15. Ansorge MS, Zhou M, Lira A, Hen R, Gingrich JA. Early-life blockade of the 5-HT transporter alters emotional behavior in adult mice. Science 2004;306:879-881.
16. Andolina D, Conversi D, Cabib S, et al. 5-Hydroxytryptophan during critical postnatal period improves cognitive performances and promotes dendritic spine maturation in genetic mouse model of phenylketonuria. Int J Neuropsychopharmacol 2011;14:479-489.
17. Durig J, Hornung JP. Neonatal serotonin depletion affects developing and mature mouse cortical neurons. Neuroreport 2000;11:833-837.
18. Dori I, Dinopoulos A, Blue ME, Parnavelas JG. Regional differences in the ontogeny of the serotonergic projection to the cerebral cortex. Exp Neurol 1996;138:1-14.
19. Vu DH, Törk I. Differential development of the dual serotoninergic fiber system in the cerebral cortex of the cat. J Comp Neurol 1992;317:156-174.
20. Wang Y, Gu Q, Cynader MS. Blockade of serotonin-2C receptors by mesulergine reduces ocular dominance plasticity in kitten visual cortex. Exp Brain Res 1997;114:321-328.
21. Moreau AW, Amar M, Le Roux N, Morel N, Fossier P. Serotoninergic fine-tuning of the excitation-inhibition balance in rat visual cortical networks. Cereb Cortex 2010;20:456-467.
22. Moreau AW, Amar M, Callebert J, Fossier P. Serotonergic modulation of LTP at excitatory and inhibitory synapses in the developing rat visual cortex. Neuroscience 2013;238:148-158.
23. Fagiolini M, Hensch TK. Inhibitory threshold for critical-period activation in primary visual cortex. Nature 2000;404:183-186.
24. Hensch TK. Critical period mechanisms in developing visual cortex. Curr Top Dev Biol 2005;69:215-237.
25. Hensch TK. Critical period plasticity in local cortical circuits. Nat Rev Neurosci 2005;6:877-888.
26. Hensch TK, Fagiolini M. Excitatory-inhibitory balance and critical period plasticity in developing visual cortex. Prog Brain Res 2005;147:115-124.
27. Katz LC, Shatz CJ. Synaptic activity and the construction of cortical circuits. Science 1996;274:1133-1138.
28. Rittenhouse CD, Shouval HZ, Paradiso MA, Bear MF. Monocular deprivation induces homosynaptic long-term depression in visual cortex. Nature 1999;397:347-350.
29. Turrigiano GG, Nelson SB. Homeostatic plasticity in the developing nervous system. Nat Rev Neurosci 2004;5:97-107.
30. Liu BH, Li P, Li YT, et al. Visual receptive field structure of cortical inhibitory neurons revealed by two-photon imaging guided recording. J Neurosci 2009;29:10520-10532.
31. Tan L, Tring E, Ringach DL, Zipursky SL, Trachtenberg JT. Vision Changes the Cellular Composition of Binocular Circuitry during the Critical Period. Neuron 2020;108:735-747.e736.
32. Maffei A, Turrigiano GG. Multiple modes of network homeostasis in visual cortical layer 2/3. J Neurosci 2008;28:4377-4384.
33. Desai NS, Cudmore RH, Nelson SB, Turrigiano GG. Critical periods for experience-dependent synaptic scaling in visual cortex. Nat Neurosci 2002;5:783-789.
34. Goel A, Lee HK. Persistence of experience-induced homeostatic synaptic plasticity through adulthood in superficial layers of mouse visual cortex. J Neurosci 2007;27:6692-6700.
35. Lempel AA, Fitzpatrick D. Developmental alignment of feedforward inputs and recurrent network activity drives increased response selectivity and reliability in primary visual cortex following the onset of visual experience. bioRxiv 2023.

36. Medini P. Cell-type-specific sub- and suprathreshold receptive fields of layer 4 and layer 2/3 pyramids in rat primary visual cortex. Neuroscience 2011;190:112-126.
37. Park SW, Jang HJ, Cho KH, Kim MJ, Yoon SH, Rhie DJ. Developmental Switch of the Serotonergic Role in the Induction of Synaptic Long-term Potentiation in the Rat Visual Cortex. Korean J Physiol Pharmacol 2012;16:65-70.
38. Hu L, Liu C, Dang M, Luo B, Guo Y, Wang H. Activation of 5-HT2A/2C receptors reduces the excitability of cultured cortical neurons. Neurosci Lett 2016;632:124-129.
39. Rao D, Basura GJ, Roche J, Daniels S, Mancilla JG, Manis PB. Hearing loss alters serotonergic modulation of intrinsic excitability in auditory cortex. J Neurophysiol 2010;104:2693-2703.
40. Jang HJ, Cho KH, Park SW, Kim MJ, Yoon SH, Rhie DJ. Layer-specific serotonergic facilitation of IPSC in layer 2/3 pyramidal neurons of the visual cortex. J Neurophysiol 2012;107:407-416.
41. Joo K, Rhie DJ, Jang HJ. Enhancement of GluN2B Subunit-Containing NMDA Receptor Underlies Serotonergic Regulation of Long-Term Potentiation after Critical Period in the Rat Visual Cortex. Korean J Physiol Pharmacol 2015;19:523-531.
42. Jang HJ, Cho KH, Park SW, Kim MJ, Yoon SH, Rhie DJ. The development of phasic and tonic inhibition in the rat visual cortex. Korean J Physiol Pharmacol 2010;14:399-405.
43. Chen XJ, Rasch MJ, Chen G, Ye CQ, Wu S, Zhang XH. Binocular input coincidence mediates critical period plasticity in the mouse primary visual cortex. J Neurosci 2014;34:2940-2955.
44. Shin D, Cho KH, Joo K, Rhie DJ. Layer-specific serotonergic induction of long-term depression in the prefrontal cortex of rats. Korean J Physiol Pharmacol 2020;24:517-527.
45. GSV, Francis-Oliveira J, Carlos-Lima E, et al. 5-HT-dependent synaptic plasticity of the prefrontal cortex in postnatal development. Sci Rep 2022;12:21015.
46. Xiang K, Zhao X, Li Y, Zheng L, Wang J, Li YH. Selective 5-HT7 Receptor Activation May Enhance Synaptic Plasticity Through N-methyl-D-aspartate (NMDA) Receptor Activity in the Visual Cortex. Curr Neurovasc Res 2016;13:321-328.
47. Huang S, Treviño M, He K, et al. Pull-push neuromodulation of LTP and LTD enables bidirectional experience-induced synaptic scaling in visual cortex. Neuron 2012;73:497-510.
48. Seol GH, Ziburkus J, Huang S, et al. Neuromodulators control the polarity of spike-timing-dependent synaptic plasticity. Neuron 2007;55:919-929.
49. Philpot BD, Espinosa JS, Bear MF. Evidence for altered NMDA receptor function as a basis for metaplasticity in visual cortex. J Neurosci 2003;23:5583-5588.
50. Dan Y, Poo MM. Spike timing-dependent plasticity of neural circuits. Neuron 2004;44:23-30.
51. Dan Y, Poo MM. Spike timing-dependent plasticity: from synapse to perception. Physiol Rev 2006;86:1033-1048.
52. Clopath C, Gerstner W. Voltage and Spike Timing Interact in STDP - A Unified Model. Front Synaptic Neurosci 2010;2:25.
53. Froemke RC, Letzkus JJ, Kampa BM, Hang GB, Stuart GJ. Dendritic synapse location and neocortical spike-timing-dependent plasticity. Front Synaptic Neurosci 2010;2:29.
54. Sugisaki E, Fukushima Y, Nakajima N, Aihara T. The dependence of acetylcholine on dynamic changes in the membrane potential and an action potential during spike timing-dependent plasticity induction in the hippocampus. Eur J Neurosci 2022;56:5972-5986.
55. Llano I, Leresche N, Marty A. Calcium entry increases the sensitivity of cerebellar Purkinje cells to applied GABA and decreases inhibitory synaptic currents. Neuron 1991;6:565-574.
56. Pitler TA, Alger BE. Postsynaptic spike firing reduces synaptic GABAA responses in hippocampal pyramidal cells. J Neurosci 1992;12:4122-4132.
57. Yoshimura Y, Ohmura T, Komatsu Y. Two forms of synaptic plasticity with distinct dependence on age, experience, and NMDA receptor subtype in rat visual cortex. J Neurosci 2003;23:6557-6566.
58. Jiang B, Huang S, de Pasquale R, et al. The maturation of GABAergic transmission in visual cortex requires endocannabinoid-mediated LTD of inhibitory inputs during a critical period. Neuron 2010;66:248-259.
59. Li YH, Xiang K, Xu X, et al. Co-activation of both 5-HT. Neurosci Lett 2018;686:122-126.
60. Roerig B, Katz LC. Modulation of intrinsic circuits by serotonin 5-HT3 receptors in developing ferret visual cortex. J Neurosci 1997;17:8324-8338.
61. Azimi Z, Barzan R, Spoida K, et al. Separable gain control of ongoing and evoked activity in the visual cortex by serotonergic input. Elife 2020;9.

62. Patel AM, Kawaguchi K, Seillier L, Nienborg H. Serotonergic modulation of local network processing in V1 mirrors previously reported signatures of local network modulation by spatial attention. Eur J Neurosci 2023;57:1368-1382.
63. Winkel F, Ryazantseva M, Voigt MB, et al. Pharmacological and optical activation of TrkB in Parvalbumin interneurons regulate intrinsic states to orchestrate cortical plasticity. Mol Psychiatry 2021;26:7247-7256.
64. Wang C, Zucker RS. Regulation of synaptic vesicle recycling by calcium and serotonin. Neuron 1998;21:155-167.
65. Seitz PK, Bremer NM, McGinnis AG, Cunningham KA, Watson CS. Quantitative changes in intracellular calcium and extracellular-regulated kinase activation measured in parallel in CHO cells stably expressing serotonin (5-HT) 5-HT2A or 5-HT2C receptors. BMC Neurosci 2012;13:25.
66. Ma WP, Liu BH, Li YT, Huang ZJ, Zhang LI, Tao HW. Visual representations by cortical somatostatin inhibitory neurons--selective but with weak and delayed responses. J Neurosci 2010;30:14371-14379.
67. Hang GB, Dan Y. Asymmetric temporal integration of layer 4 and layer 2/3 inputs in visual cortex. J Neurophysiol 2011;105:347-355.
68. Yang W, Carrasquillo Y, Hooks BM, Nerbonne JM, Burkhalter A. Distinct balance of excitation and inhibition in an interareal feedforward and feedback circuit of mouse visual cortex. J Neurosci 2013;33:17373-17384.
69. Bruno RM. Synchrony in sensation. Curr Opin Neurobiol 2011;21:701-708.
70. Hage TA, Bosma-Moody A, Baker CA, et al. Synaptic connectivity to L2/3 of primary visual cortex measured by two-photon optogenetic stimulation. Elife 2022;11.
71. Packer AM, Yuste R. Dense, unspecific connectivity of neocortical parvalbumin-positive interneurons: a canonical microcircuit for inhibition? J Neurosci 2011;31:13260-13271.
72. Adesnik H, Bruns W, Taniguchi H, Huang ZJ, Scanziani M. A neural circuit for spatial summation in visual cortex. Nature 2012;490:226-231.
73. Fino E, Packer AM, Yuste R. The logic of inhibitory connectivity in the neocortex. Neuroscientist 2013;19:228-237.
74. Cardin JA. Snapshots of the Brain in Action: Local Circuit Operations through the Lens of γ Oscillations. J Neurosci 2016;36:10496-10504.
75. Atallah BV, Scanziani M. Instantaneous modulation of gamma oscillation frequency by balancing excitation with inhibition. Neuron 2009;62:566-577.
76. Adesnik H. Layer-specific excitation/inhibition balances during neuronal synchronization in the visual cortex. J Physiol 2018;596:1639-1657.
77. Fries P. Neuronal gamma-band synchronization as a fundamental process in cortical computation. Annu Rev Neurosci 2009;32:209-224.
78. Adesnik H, Scanziani M. Lateral competition for cortical space by layer-specific horizontal circuits. Nature 2010;464:1155-1160.
79. Ozeki H, Finn IM, Schaffer ES, Miller KD, Ferster D. Inhibitory stabilization of the cortical network underlies visual surround suppression. Neuron 2009;62:578-592.
80. Jadi MP, Sejnowski TJ. Cortical oscillations arise from contextual interactions that regulate sparse coding. Proc Natl Acad Sci U S A 2014;111:6780-6785.
81. Jadi MP, Sejnowski TJ. Regulating Cortical Oscillations in an Inhibition-Stabilized Network. Proc IEEE Inst Electr Electron Eng 2014;102.
82. Xu X, Olivas ND, Ikrar T, et al. Primary visual cortex shows laminar-specific and balanced circuit organization of excitatory and inhibitory synaptic connectivity. J Physiol 2016;594:1891-1910.
83. Jiang B, Treviño M, Kirkwood A. Sequential development of long-term potentiation and depression in different layers of the mouse visual cortex. J Neurosci 2007;27:9648-9652.
84. Dyck RH, Cynader MS. Autoradiographic localization of serotonin receptor subtypes in cat visual cortex: transient regional, laminar, and columnar distributions during postnatal development. J Neurosci 1993;13:4316-4338.
85. Maya Vetencourt JF, Tiraboschi E, Spolidoro M, Castrén E, Maffei L. Serotonin triggers a transient epigenetic mechanism that reinstates adult visual cortex plasticity in rats. Eur J Neurosci 2011;33:49-57.
86. Maya-Vetencourt JF, Tiraboschi E, Greco D, et al. Experience-dependent expression of NPAS4 regulates plasticity in adult visual cortex. J Physiol 2012;590:4777-4787.

87. Baroncelli L, Sale A, Viegi A, et al. Experience-dependent reactivation of ocular dominance plasticity in the adult visual cortex. Exp Neurol 2010;226:100-109.
88. Balog J, Matthies U, Naumann L, Voget M, Winter C, Lehmann K. Social experience modulates ocular dominance plasticity differentially in adult male and female mice. Neuroimage 2014;103:454-461.
89. Edagawa Y, Saito H, Abe K. The serotonin 5-HT2 receptor-phospholipase C system inhibits the induction of long-term potentiation in the rat visual cortex. Eur J Neurosci 2000;12:1391-1396.
90. Kim HS, Jang HJ, Cho KH, et al. Serotonin inhibits the induction of NMDA receptor-dependent long-term potentiation in the rat primary visual cortex. Brain Res 2006;1103:49-55.
91. Edagawa Y, Saito H, Abe K. Stimulation of the 5-HT1A receptor selectively suppresses NMDA receptor-mediated synaptic excitation in the rat visual cortex. Brain Res 1999;827:225-228.
92. Athilingam JC, Ben-Shalom R, Keeshen CM, Sohal VS, Bender KJ. Serotonin enhances excitability and gamma frequency temporal integration in mouse prefrontal fast-spiking interneurons. Elife 2017;6.
93. Andrade R. Serotonergic regulation of neuronal excitability in the prefrontal cortex. Neuropharmacology 2011;61:382-386.
94. Durieux LJA, Gilissen SRJ, Arckens L. Endocannabinoids and cortical plasticity: CB1R as a possible regulator of the excitation/inhibition balance in health and disease. Eur J Neurosci 2022;55:971-988.
95. Kim HH, Park JM, Lee SH, Ho WK. Association of mGluR-Dependent LTD of Excitatory Synapses with Endocannabinoid-Dependent LTD of Inhibitory Synapses Leads to EPSP to Spike Potentiation in CA1 Pyramidal Neurons. J Neurosci 2019;39:224-237.
96. Crosby KM, Inoue W, Pittman QJ, Bains JS. Endocannabinoids gate state-dependent plasticity of synaptic inhibition in feeding circuits. Neuron 2011;71:529-541.